Oikonomou *et al. Earth, Planets and Space* (2023) 75:39
https://doi.org/10.1186/s40623-023-01796-6

Earth, Planets and Space

FULL PAPER

Open Access

Occurrence features of intermediate descending layer and Sporadic E observed over the higher mid-latitude ionospheric station of Moscow

Christina Oikonomou[1*], Theodoros Leontiou[1,2], Haris Haralambous[1,2], Tamara L. Gulyaeva[3] and V. A. Panchenko[3]

Abstract

Nine years of ionograms from a higher mid-latitude ionospheric station (Moscow) are analyzed, by applying the 'height–time–intensity' (HTI) technique along with Spectrum (Lomb periodogram) analysis with the aim to investigate the daily and seasonal variability of sporadic E (Es) and intermediate descending layers (IDLs). Es and IDL traces are observed over Moscow, which are characterized by a 12-h periodicity prevailing throughout the year. Shorter periodicities in IDL and Es occurrence are also observed. A 6-h periodicity in Es and IDL dominates during November and December, while an 8-h periodicity is found mainly from October to February for IDL and in July for Es. These periodicities are primarily induced by the semi-, quarter- and terdiurnal thermospheric tides, respectively. Our results also establish the systematic and widespread manifestation of shorter-scale (4.8- and 4-h) periodicities observed mainly for IDL and less frequently for Es only during December and January, in the nine years considered, which is most probably linked to higher-order solar tides.

Keywords Intermediate descending layer, Sporadic E, Thermospheric tides

*Correspondence:
Christina Oikonomou
res.ec@frederick.ac.cy
Full list of author information is available at the end of the article

Graphical Abstract

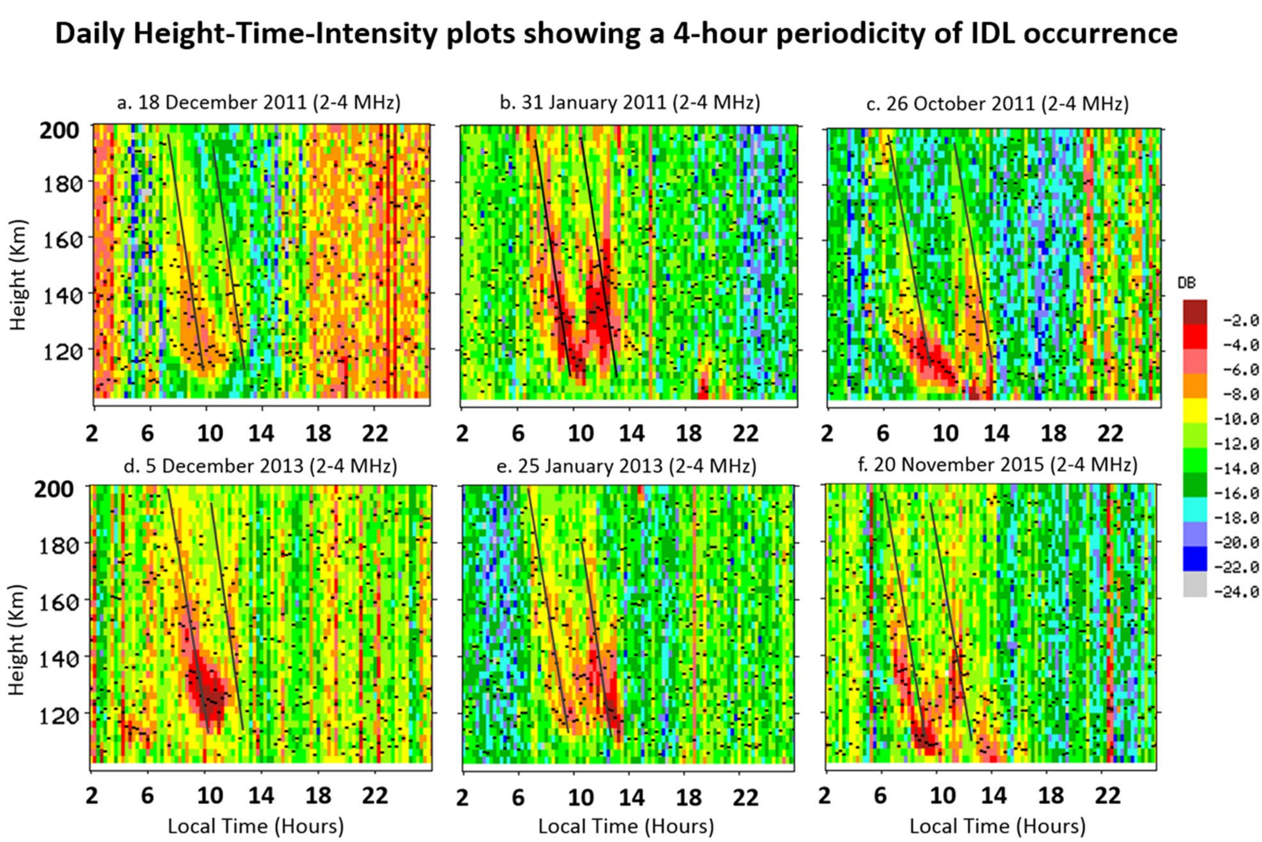

Introduction

Intermediate Descending Layers (IDLs) are weak but long-lived ionization layers which detach from the bottomside of the F region (~ 200 km) and move downwards (conveying metal ions) to gradually merge with Sporadic E layers (Es) below at ~ 120 km, thus they constitute the main generating process for Es (Haldoupis 2012). Intermediate layers may be consisting of molecular ions such as NO^+ and $O2^+$, metallic ions such as Fe^+ and Mg^+, or combinations of both. It is most probable that when IDLs form, they are comprised entirely of molecular ions, but as they descend their composition evolves with an increasing percentage of metallic ions present (Earle et al. 2000). Sporadic E layers are comprised almost solely of metallic ion plasma mainly between 100 and 130 km in the mid-latitude ionosphere. Their thickness is of about 1–2 km and their horizontal length is tens to hundreds of km (Maeda and Heki 2014).

The formation mechanism of IDL and Es is most readily explained by the wind shear theory (WST) (Whitehead 1961; Axford 1963) which involves a combination of neutral wind fields and geomagnetic field geometry. Properly oriented vertical wind shears of the horizontal neutral wind are necessary to cause long-living metallic ions to move downwards and converge into thin ionization layers. Such wind shear convergence nodes are mainly controlled by thermospheric tides. An interpretive description of the WST is provided by Haldoupis (2012). The main drawback, of the WST is that it cannot explain the formation and evolution of IDL and Es in regions other than mid-latitude regions. Es generation should be inhibited on the magnetic equator, since the horizontal magnetic field does not allow the ions to converge vertically into a layer (Yu et al. 2019). Over the equatorial regions, Es_q layers in the ionograms are formed from the gradient instability caused by the equatorial electrojet current (Resende et al. 2022; Li et al. 2013), while atmospheric gravity waves (AGWs) and electric fields concentrate the ionization of Es layers over high magnetic latitudes (polar caps) (MacDougall et al 2000, 2005). Recently, Qiu et al. (2021) reported that Es traces observed by ionosondes located at mid-latitude regions and the wind shear convergence nodes derived from simulations do not completely overlap in the vertical direction, which implies that WST cannot fully explain the vertical evolution of Es, thereby, the joined effect of wind shear, metallic ion distribution and AGWs should be also taken into consideration. Didebulidze et al. (2020) demonstrated theoretically and numerically the formation of multilayered Es by AGWs propagating in the mid-latitude lower thermosphere.

Sporadic E morphology and variability have been intensively studied over the past six decades, in particular over the low- and mid- latitude regions (Bencze et al. 2004; Christakis et al. 2009; Pietrella and Bianchi 2009; Voiculescu et al. 1999; Yeh et al. 2014; Pignalberi et al. 2014; Mozna et al. 2015; Pezzopane et al. 2015; Haldoupis et al. 2020), however, radio occultations allowed a thorough mapping of the global Es morphology. Yu et al. (2020) used Radio Occultation (RO) profiles from the FORMOSAT-3/COSMIC satellite mission to study the global distribution of Es critical frequency (foEs) with a high spatial resolution ($1^\circ \times 1^\circ$), while Gan et al. (2022) studied the seasonal variations of Es on a global scale using the first RO soundings obtained from the China Seismo-Electromagnetic Satellite (CSES). RO-observed Es layers from COSMIC and Fengyun-3C (FY-3C) missions were intercompared globally and found to be consistent, though, with slight differences (Xu et al. 2022). In addition, Saito et al. (2021) identified fine structures (such as the sub-structures in the Es layer front) by utilizing total electron content (TEC) index (ROTI) maps with dense Global Navigation Satellite System (GNSS) observations over Japan.

Unlike Sporadic E, less emphasis has been placed to date into IDL characteristics. The first observations of IDLs were obtained from the Incoherent Scatter Radar (ISR) located at the Arecibo station (MacDougall 1974; Rowe 1974; Tong et al. 1988; Mathews et al. 1993; Morton et al. 1993; Osterman et al. 1994) which revealed the tidal motion and seasonal variations of IDLs over low-latitudes. Numerical simulations by Andoh et al. (2022) successfully reproduced for the first time day-to-day variations of the observed Es layers at Arecibo, while the same authors have also presented the first simulations of midlatitude Es day-to-day variability (Andoh et al. 2020). Recently, Santos et al. (2019, 2020 & 2022) focused on the occurrence peculiarities, the response on solar activity and the climatology of IDL over several low-latitude stations in Brazil. They identified nocturnal IDLs and, interestingly, ascending intermediate layers which were attributed to upward propagating AGWs. They also demonstrated that even small variations in the geomagnetic activity during low solar activity can affect the height and frequency of IDLs. Their results also confirmed that thermospheric tides (diurnal, semidiurnal, terdiurnal and quarter-diurnal) are the principal causal mechanism behind IDL formation. Only a few studies have been conducted over the equator and sub-tropics (Niranjan et al. 2010; Lee et al. 2003; Patra 2011). The effect of such type of thermospheric tides on the formation of IDLs and Es has been also identified over mid-latitudes (Haldoupis et al. 2007; Pietrella et al. 2009; Haldoupis & Pancheva 2006; Oikonomou et al. 2014). Arras et al. (2009) evaluated semidiurnal tidal signature in Es occurrence rate at higher mid-latitude regions.

The majority of previous studies focused only on lower-order tidal periodicities in Es and IDL occurrence (12-, 8-, 6- hour), except Earle et al. (2000), who detected systematically multiple ionisation layers rapidly descending from ~ 170 km within intervals of only a few hours (~ 2 h) at the low-latitude Arecibo ISR, indicating shorter IDL periodicities. They attributed the rapid descend of these layers to higher-order tidal modes in thermospheric winds. These tides have received little attention by the scientific community so far. Only minor studies have shown the predominance of higher-order tidal oscillations in lower thermospheric and upper mesospheric temperature over high-latitude regions (Won et al. 2003; Smith et al. 2004 and Walterscheid G. G. Sivjee, 1996).

More recently, Oikonomou et al. (2022) concentrated on the Es and IDLs tidal variability and occurrence over several mid-latitude European stations. Their results confirmed the well-established tidal patterns of Es and IDLs traces characterized by the 12-, 8- and 6-h periodicity, and notably, revealed the systematic appearance of a 4-h IDL periodicity in winter months only over higher mid-latitude stations. The present study is a continuation of this investigation, with the aim to confirm and establish the systematic manifestation of both higher- and shorter-scale IDL and Es periodicity over higher mid-latitudes, attempting also to understand and explain their origin and characteristics.

On this basis, we examine the characteristics and the seasonal variations of IDL and Es over a higher mid-latitude ionosonde station in Moscow, by analyzing an extended database of ionograms by exploiting the height-time-reflection intensity (HTI) technique and Spectrum analysis (Lomb normalized periodogram). Moscow station was selected as it is located relatively close to the three higher mid-latitude European stations Pruhonice (50°N, 14.6°E), Dourbes (50.1°N, 4.6°E), and Juliusruh (54.6°N, 13.4°E), that have been examined at our previous work (all fours stations have almost the same latitude and they are located within the longitude window 4° to 37° E). Furthermore, only two studies were dedicated on Es

(Yusupov et al. 2021; Maksyutin et al. 2001) and no one on IDL over Moscow.

Data and methodology

Our investigation utilizes ionograms, during a 9-year period (2011–2019) from a Digisonde (DPS-4) station located near Moscow (55.47°N, 37.30°E) which can be accessed from the DIDBase (Digital Ionogram Database, https://ulcar.uml.edu/DIDBase/) of the Global Ionospheric Radio Observatory (GIRO, http://giro.uml.edu/). DPS-4D Digisonde is an advanced ionospheric sounder which performs ionogram recordings every 15 min using the Digisonde Precision Group Height Measurement (PGHM) technique (Reinisch et al. 2008). The ionosonde can receive reflections from heights where electron densities exceed ~ 1.24×10^4 cm^{-3}, considering that its lowest transmission frequency is 1 MHz.

The HTI method, introduced by Haldoupis et al., (2006) and employed by the World Data Center for the Ionosphere (https://wdc.nict.go.jp/cgi-bin/ionog/sum_control.cgi) for more than 35 years, is used to identify tide-like variations in Es and IDLs. It applies on an individual ionogram, which represents a snapshot of the reflected signal intensity (in dB) as a function of (virtual) height and ionosonde frequency, focusing on a fixed frequency bin of the ionogram. The process is repeated on consecutive ionograms so that an HTI plot is obtained for a certain frequency bin. Since we are interested in tidal periodicities in Es and IDL, a 24-h local time axis is used for the HTI plots, which can be time averaged over a selected time interval, for instance over a week or a month. In this study, representative monthly average HTI plots for the period 2011–2019 were used.

We also apply spectrum analysis for the same period aiming to quantify the observed (from HTI plots) occurrence of Es and IDL periodicities and consolidate their seasonal variability. More specifically, the Lomb normalized periodogram as described in Press et al. (2007) is applied on the numerical data (virtual height of ionospheric layers) retrieved from the ionograms for the period under investigation. This method estimates the harmonic content of a dataset, at a given frequency in an equivalent way to the linear least-squares fitting to the model. It also allows data with missing points to be analyzed without the need of interpolation. We apply the method twice, using the height intervals, 100–140 km and 150–220 km, for Es and IDL traces respectively. The frequency bin 1.5–4 MHz is selected to capture Es and 1DL periodicities, based on our experience gained from the inspection of all ionograms over Moscow during the period under examination.

Results and discussion

The diurnal and seasonal occurrence features of IDL and Es over Moscow station are investigated for the period 2011–2019 with the ultimate aim to ascertain the dominant long-term tide-like variability as well as the altitude descent patterns in Es and IDL traces over the higher mid-latitude regions. For this purpose, average daily HTI plots for each month are produced.

Mean diurnal and seasonal characteristics in Es and IDL occurrence

In Fig. 1, representative average daily HTI plots for each month of the year are presented. In all months, a semidiurnal pattern of two Es layers prevails. These two layers, appear at sunrise and afternoon (~ 16 LT) near 120 km, and descend steadily reaching down to ~ 100 km in approximately 12 h with a sloping rate of ~ 2 km/h. This semidiurnal periodicity in Es layers is found during the whole year (for all 9 years concerned), albeit with notable differences in their intensity per season. In particular, from February to April strong semidiurnal Es traces (mainly in daytime and less in nighttime) are detected in the lower E region (Figs. 1c–e) which intensify during summer months (May to August) both in day and night (Figs. 1f–i). This semidiurnal pattern in Es occurrence becomes less pronounced in September and October) (Fig. 1j, Figure not shown for October) and continues to weaken in winter months December and January) (Figure not shown) most probably due to lower ambient metal ion density during winter months (Shinagawa et al. 2021). Es intensity is discussed in the following section.

A semidiurnal periodicity is also identified in the IDLs occurrence, which initiate near sunrise at the bottom of the F layer (~ 220 km) and move constantly downwards within 10 to 12 h to merge with Es layer (Fig. 1). This semidiurnal pattern in IDL traces is reinforced mainly from February to May (Figs. 1c–e) and is weaker during September to November (Figs. 1j–l), while it almost disappears from May to August (Figs. 1f–i) and weakens in December and January (Figure not shown). The disappearance of the summer IDL is due to the intensified Es layers observed during summer, which are blanketing the ionosonde reflections from the F layer and thus prevent the detection of daytime IDLs above. However, the application of Spectrum analysis allowed the IDL detection not only in summer, but also during all seasons as well, as it will be discussed in the following section. Furthermore, the appearance of daytime and nighttime IDLs has been confirmed over the low latitudes with the aid of Arecibo ISR (Mathews 1998). The nighttime IDL was not observed in our HTI analysis, as it was too weak to be detected by ionosonde, which can observe layers with

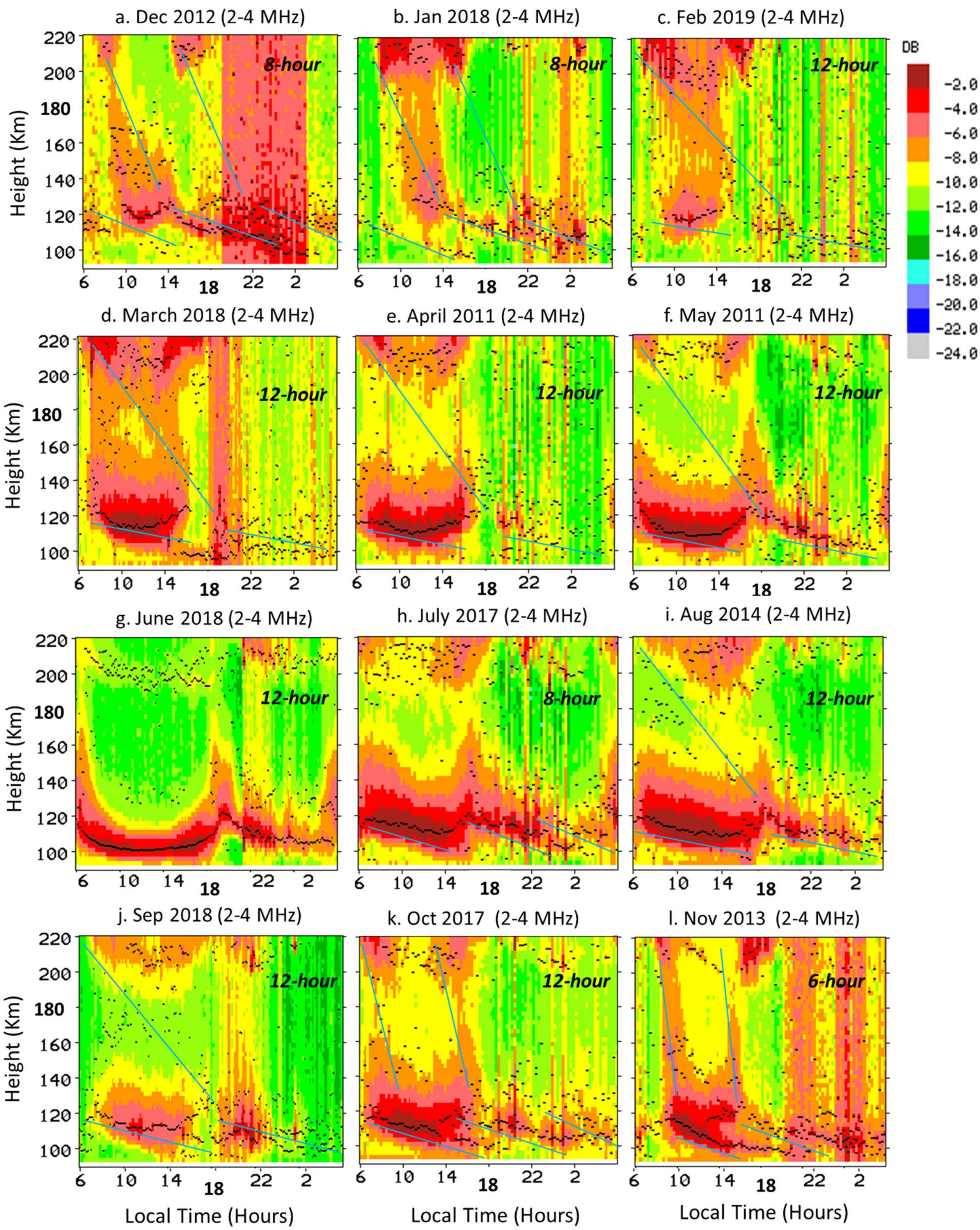

Fig. 1 Representative average HTI plots in Moscow for: **a** December, **b** January, **c** February, **d** March, **e** April, **f** May, **g** June, **h** July, **i** August, **j** September, **k** October and **l** November. The frequency band used for each plot is 2–4 MHz. Light blue lines are drawn to help the reader identify easier IDLs and Es descent. The observed periodicity of IDLs and Es oscillations for each month is also written on the top right of each panel

electron density greater than 1.24×10^4 cm^{-3}. Because of the absence of photoionization, ambient ions (mainly O^+) are reduced during night; therefore, the layers forming in the F region are weaker comparing with the daytime layers. At lower heights (E region) the concentration of metal ions available for layer formation during day is largest than that during night (Haldoupis et al. 2007).

The observed 12-h periodicity in Es and IDLs occurrence is consistent with the results of previous studies (Haldoupis 2012; Pignalberi et al. 2014; Oikonomou et al. 2014, 2022) and is attributed to the downward phase propagation of the semidiurnal tides which dominate in the thermosphere throughout the year (Forbes 1995). Apart from the prevailing semidiurnal periodicity, a terdiurnal periodicity is evident for winter months October, December, and January in IDL and Es (Figs. 1a, b, k) and during July (Figs. 1h) only for Es. As it can be seen in Figs. 1a and b, during December and January the daily pattern of this terdiurnal periodicity is characterized by three apparent Es layers, starting at an altitude of 120 km moving downwards to 100 km. The first layer appears around sunrise (~ 8 LT), the second at noon (~ 16 LT) and the last one at night (~ 24 LT). At the same time, two intermediate descending layers detach from the bottomside of the F layer (at ~ 220 km) and move downwards, within 8 h apart, to finally connect with the Es layer at about 120 km. During summer, however, these IDLs were impossible to detect as explained earlier. This 8-h periodicity in Es and IDL traces was observed also during autumn and spring, though with much less intensity, with the aid of Spectrum analysis (see Sect. "Quantitative analysis of IDL and Es occurrence"), despite the fact that is not evident in the respective HTI plots. A similar terdiurnal periodicity in Es was reported earlier over lower mid-latitude ionosonde stations (Nicosia in Cyprus, Milos and Athens in Greece) during summer (Haldoupis et al. 2004; Oikonomou et al. 2014, 2022), as well as less frequently over the higher mid-latitude ionosonde station Pruhonice in Czech Republic by Mosna et al. (2015). It has been demonstrated that the terdiurnal thermospheric tides are behind the formation of the 8-h periodicity in IDL and Es (Haldoupis, and Pancheva 2006) while the fact that the terdiurnal pattern in ionospheric layers are weaker than the semidiurnal one, is most probably due to the fact that terdiurnal tides are not as strong as semidiurnal tides at higher mid-latitudes to drive the formation of IDL and Es (Jacobi 2012; Azeem et al. 2016).

Another shorter (6-h) periodicity in IDL and Es occurrence is also detected by HTI during November (Fig. 1l) and December (Figure not shown). As it can be seen in Fig. 1l, two IDLs are initiate from the bottomside of the F layer (~ 210 km) at 6 h apart, the first at ~ 8 LT and the second at ~ 14 LT. They both descend rapidly in approximately 2 h to finally merge with the Es layers below at ~ 130 km, with a velocity of ~ 40 km/h. Es layers subsequently intensify, also six hours apart, the first at ~ 10 LT and the next one at ~ 16 LT, while they continue to move downwards from ~ 130 km to ~ 100 km within six hours with a much slower descending rate of around 5 km/h.

Our results are consistent with previous studies that reported a similar quarter-diurnal periodicity in Es and IDLs over lower mid-latitude regions (Pignalberi et al 2014; Haldoupis and Pancheva 2006) and higher mid-latitudes (Oikonomou et al. 2022). The systematic appearance of the quarter-diurnal periodicity in Es and IDLs was also reported over equatorial and low latitude regions (Tong et al. 1988; Carter and Forbes 1999; Earle et al. 2000; Niranjan et al. 2010; Christakis et al. 2009), and was attributed to the quarter-diurnal thermospheric tides, which though weaker than the semidiurnal and terdiurnal tides they are also a major contributor to the ionospheric-thermospheric dynamics (Kumari, 2021). Despite this 6-h periodicity primarily observed during November and December, the combined analysis of HTI and Spectrum results that are presented in the next section, identify this periodicity during spring months as well, with a much lower intensity.

Quantitative analysis of IDL and Es occurrence

The HTI plots clearly demonstrated the seasonal variations both in frequency and intensity of the observed IDL and Es periodicities. The intensity of these periodicities is quantified here by applying Spectrum analysis (Lomb normalized periodogram) on the numerical data retrieved from ionograms over Moscow station during the period concerned.

In Fig. 2, the Lomb normalized periodograms concerning Es periodicity over for Moscow station for the 9-year period 2011–2019 are illustrated on a monthly basis. As it can be seen, the semidiurnal periodicity in Es prevails over all seasons while it is more pronounced in February, March, July and August and less in winter months. These findings are in compliance with the respective HTI results. The terdiurnal periodicity in Es is also observed within all seasons, though it is not as strong as the semidiurnal one. In particular, the terdiurnal Es periodicity intensifies during July and August whereas it is weaker in rest of the months. During September and October, the quarter-diurnal periodicity in Es is found to be stronger than the 8-h periodicity, which is in agreement with the respective HTI findings. Though faint enough, the quarter-diurnal periodicity in Es is also present within the rest months of the year as well.

Similarly, the monthly Lomb normalized periodograms are produced for IDL periodicity for the same period.

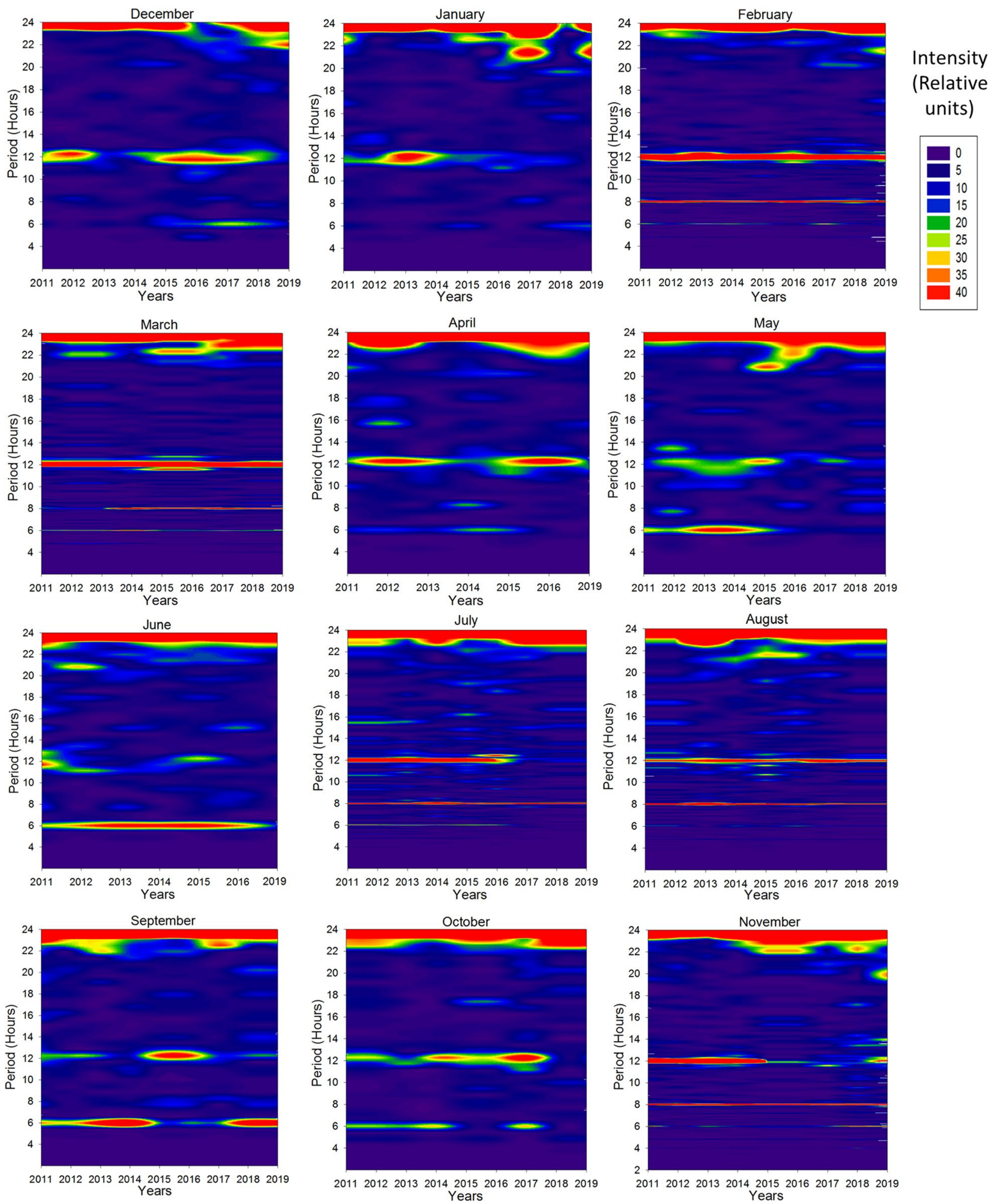

Fig. 2 Lomb periodograms of ionogram numerical data corresponding to Es over Moscow. The observed periodicities on Es occurrence for each month for the period 2011–2019 are shown

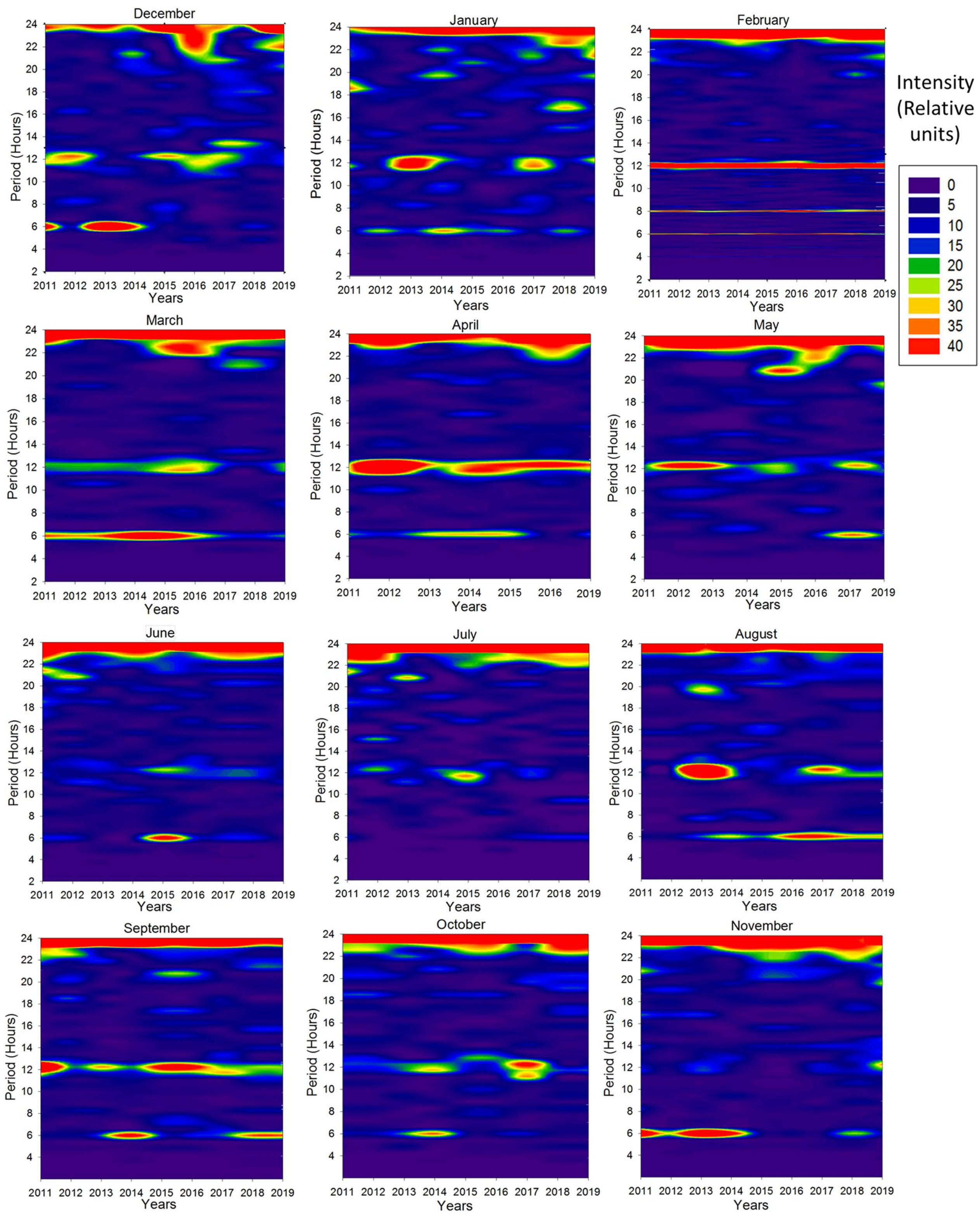

Fig. 3 Lomb periodograms of ionogram numerical data corresponding to IDLs over Moscow. The observed periodicities on Es occurrence for each month for the period 2011–2019 are shown

The results are shown in Fig. 3. The semidiurnal periodicity in IDL occurrence predominates from February to April) and during September and October, which is consistent with the HTI results as well as with previous mid-latitude studies (Oikonomou et al. 2014, 2022). This prominent feature during equinoctial months and mainly in Spring equinox, is most probably associated with the amplification of semidiurnal thermospheric tides during this season (Forbes and Vial 1989; Oberheide et al. 2011) and the possible enhancement of the bottomside F region electron density during spring (Yamazaki and Richmond 2013). The semi-diurnal periodicity in IDL becomes less intense in November, December, and January and it greatly attenuates in June and July due to blanketing Es layers at lower altitudes. The terdiurnal periodicity in IDL is considerably weaker during all months, except December and January where it appears slightly stronger, in accordance with the corresponding mean monthly HTI plots. It is also found much less intense compared to the quarter-diurnal periodicity in IDL throughout the year. The quarter-diurnal IDL periodicity is more intensified during winter and autumn months (mainly in December, January, and November however, it is also appearing during spring and summer months (mainly in March, April, August and September).

Apart from the dominant 12-, 8- and 6- hour periodicities in Es and IDL occurrence which are present during the whole year, shorter periodicities in IDL an Es are revealed in the Lomb periodograms (4- and 4.8- hour) which have not been substantiated and fully described in the literature. For this reason, the following section is devoted on the occurrence characteristics, the seasonal variability and the possible casual physical mechanisms of these shorter periodicities. A 24-h periodicity on both IDL and Es which, as seen in Figs. 2 and 3, persists in all months during the 9-year period under investigation, has also been reported by other authors, who attributed them to the 24-h solar atmospheric tides (Pietrella et al. 2014; Christakis et al. 2009).

Shorter-scale (4- and 4.8- hour) periodicities in IDL and Es occurrence

In a recent study on IDL and Es occurrence characteristics over mid-latitude regions, we demonstrated the systematic manifestation of a shorter (4-h) periodicity mainly in IDL during winter over three higher mid-latitude stations in Europe (Oikonomou et al. 2022). This section extends that investigation and concentrates to the new evidence of this short-scale periodicity over Moscow station. The application of the HTI analysis for the 9-year period 2011–2019 reveals, apart from the well-established 12-, 8- and 6-h periodicities in IDL and Es descending motion, the systematic appearance of even shorter-scale (4- and 4.8- hour) periodicities during December and January and their occasional appearance during February and November.

Figure 4 shows typical examples of HTI daily plots during several days in December, January, November and October where shorter-scale periodicities are identified. More specifically, two rapidly downward moving IDLs are shown to occur with four hours apart, the first one starting ~ 200 km at sunrise (~ 8:00 LT) and descending to the altitude of ~ 110 km within two hours, with an approximate velocity of 45 km/h. The second one detaches about four hours later at (~ 12:00 LT) from the bottomside of the F layer and moves rapidly downwards at ~ 110 km with a similar descending rate. These observations are consistent with our previous findings concerning the higher mid-latitude European stations Dourbes (50.1°N, 4.6°E), Juliusruh (54.6°N, 13.4°E) and Pruhonice (50°N, 14.6°E). Figure 5 demonstrates the steady downward progression of the two rapidly descending layers within a typical day. More specifically, it presents successive ionograms during 18 December 2011 at certain times, starting from sunrise until noon. Within this interval, the downward movement of two IDLs is clearly seen, with the first layer initiating at ~ 8:00 LT and the second one, four hours later.

The rate of occurrence of the observed 4-h periodicity mainly during December and January (estimated as the number of days within a month showing a 4-h IDL periodicity) was also calculated. It is found that this short-scale periodicity is present at 10 days per month on average (taking into account the number of missing days during each month) pointing out to a systematic and not occasional phenomenon. As illustrated in Fig. 6, the number of days with a 4-h periodicity during January ranges from 3 to 15 days.

The application of HTI analysis for a long-term period (9 years) as well as the visual inspection of the 9-year ionogram database over Moscow clearly declare that the 4-h periodicity mainly in IDL is a common phenomenon during December and January, and rarely during February and November. To consolidate this new finding, we applied the spectrum analysis (Lomb periodogram) on the numerical data deriving from the ionograms records for each winter of the examined period. The results are illustrated in Fig. 7 where the 4-h periodicity in IDL occurrence is distinctly identified. Though it appears weaker than the 24-, 12-, 8- and 6-h periodicities, it is found to occur during December and January in all nine years, in agreement also with the HTI findings, reinforcing the conclusion that it comprises a persistent phenomenon during these winter months. In addition, another weak but insistent short-scale (4.8-h) periodicity in IDL is evident in the Lomb periodogram (Fig. 7) throughout

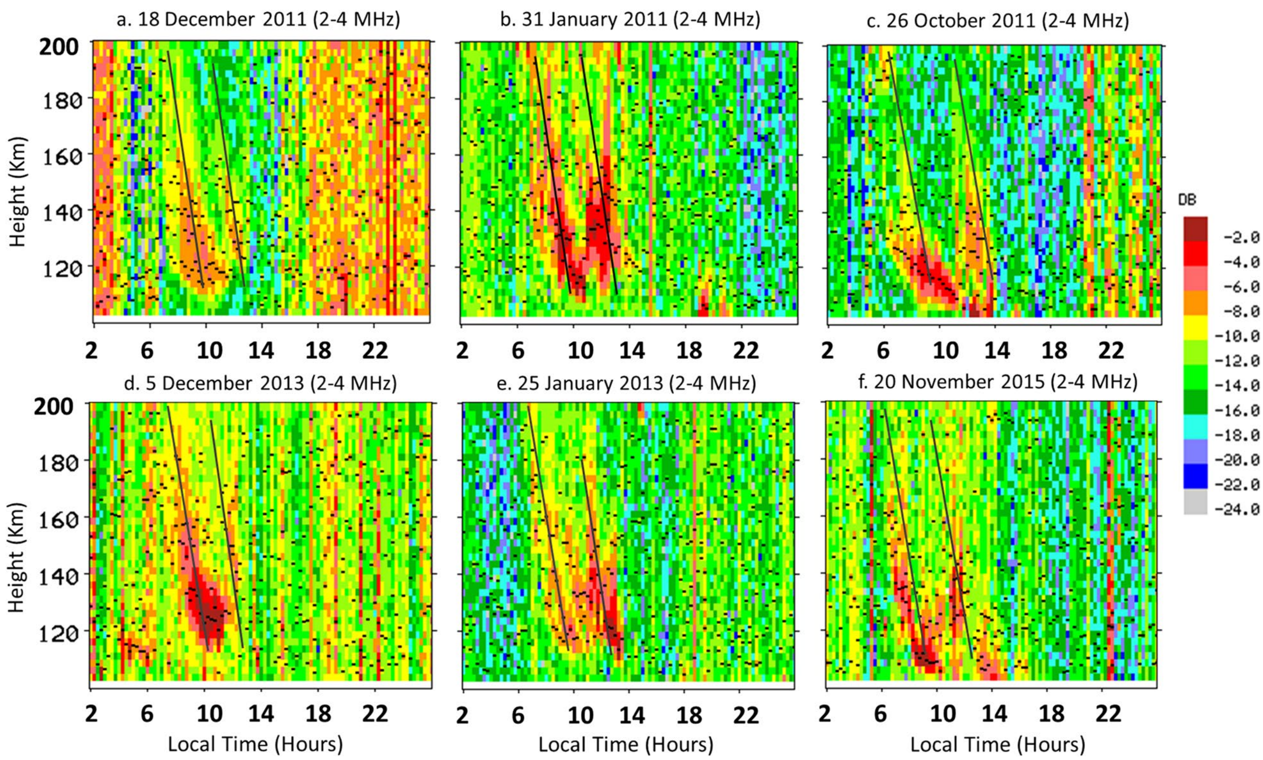

Fig. 4 Examples of daily HTI plots showing a 4-h periodicity of IDL occurrence over Moscow station during: **a** 18 December 2011, **b** 31 January 2011, **c** 26 October 2011, **d** 5 December 2013, **e** 25 January 2013 and **f** 20 November 2015. Dark solid lines are drawn to help the reader identify the IDLs altitude descent

the same period of the year, which is also observed at the respective daily HTI plots.

As it is known, solar atmospheric tides exhibit periodicities equal to the solar day and its sub-harmonics (24, 12, 8, 6, 4.8, 4-h etc.) (Taylor et al. 1999). The persistence of the shorter periodicities (4- and 4.8- hour) mainly in IDLs and less frequently in Es over four higher mid-latitude stations (Moscow, Pruhonice, Juliusruh and Dourbes) during December and January throughout a long period (9 years for Moscow and 5 years for the rest three stations) urges us to relate their occurrence primarily to higher-order solar tides in the upper thermosphere. The average monthly as well as the daily HTI plots of all four stations which are located at approximately the same latitude covering a longitudinal range of about 2500 km, demonstrated that IDLs occur at two specific times of the day, around local sunrise (8 LT) and four hours later (~ 12 LT) during the long-term period under investigation. This supports that the 4-h periodicity in IDL is a global-scale phenomenon. In addition, these tidal-like oscillations start about 2 h earlier over the most eastern station Moscow than the other 3 European stations, suggesting that observed tide-like oscillations might be due to solar migrating tides propagating westward. Because of their short periods, these tides have large vertical wavelengths, which allow them to propagate vertically into very high altitudes in the upper thermosphere (Smith and Ortland 2001). In Fig. 8, daily HTI plots for 31 January 2015 are presented for the three longitudinally separated stations of Dourbes, Pruhonice and Moscow. A 4-h IDL periodicity is apparent, characterized by two descending layers, first appearing at an altitude of 220 km, the first around 8 UT and the second four hours later (~ 12UT). In support to our postulation, gravity waves that may also contribute in the period range between 4 and10 h, should be cancelled out in monthly averaged HTI plots due to their random periodicities (Liu et al. 2020).

Additionally, Miyoshi et al. (2009) showed that solar terminator (ST) waves in the upper thermosphere are mainly generated by the superposition of upward propagating higher-order migrating tides (6-, 4.8- and 4-h period). Using a general circulation model (GCM) they demonstrated that the amplitude of these higher-order tides (manifested as temperature and horizontal wind tidal fluctuations) is maximized at the heights 150 to 400 km, while below 150 km, it starts to decrease as the height decreases. They also found that these ST waves are more pronounced during solstice. Their results, which were consistent with CHAMP and SABER satellite observations, reinforce our hypothesis that the shorter period

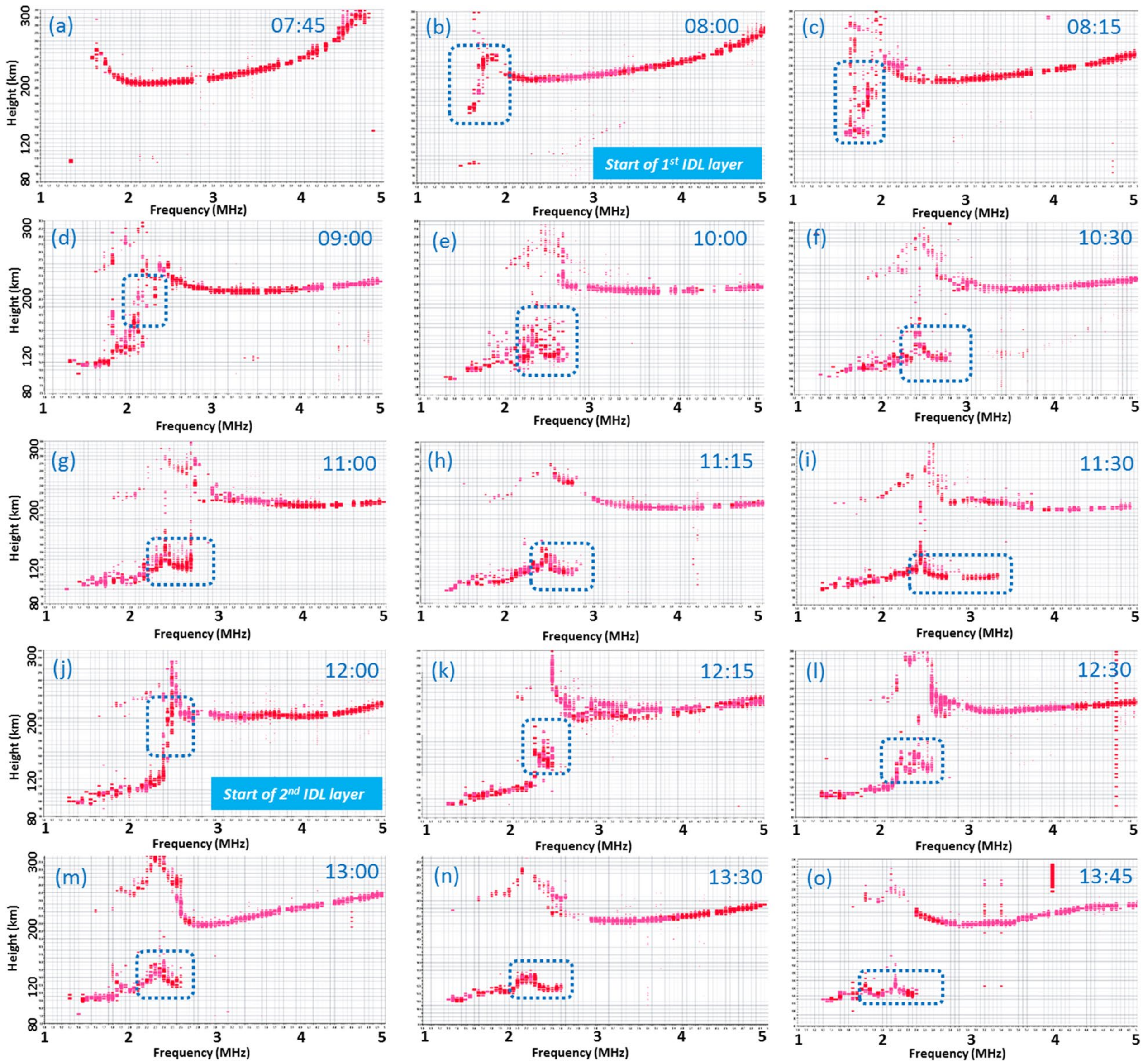

Fig. 5 Ionogram plots at successive times (LT): **a** 7:45, **b** 8:00, **c** 8:15, **d** 9:00, **e** 10:00, **f** 10:30, **g** 11:00, **h** 11:15, **i** 11:30, **j** 12:00, **k** 12:15, **l** 12:30, **m** 13:00, **n** 13:30 and **o** 13:45, during 18 December 2011 in Moscow station showing the downward movement of 2 IDLs. The 1st IDL starts at 8:00 LT and the 2nd four hours later at 12:00 LT, indicating a 4-h periodicity in IDL occurrence. IDL traces are indicated with blue dotted boxes

tide-like oscillations of IDL observed at a similar height range (~110–200 km) over Moscow near local sunrise during December, January and February might also be associated to higher-order solar tides.

In a recent study, also, He et al. (2020), by combining mesospheric wind measurements from three higher mid-latitude meteor radars (of ~55°N longitude) during two months before and after the onset of twelve sudden stratospheric warming (SSW) events within the interval 2008–2018, verified the amplification (in terms of intensity and frequency) of high-order solar migrating atmospheric tides several days (up to 50 days) before the onset of each winter SSW event and their quenching after the event. Taking into consideration that the three meteor radars are located at similar longitudes with the four selected ionospheric stations (in Juliusruh station a meteor radar and a ionosonde radar coexist) and the fact that the onset of the selected SSW events occurred towards the end of January or beginning of February, we believe that the short tidal periodicities of ionospheric layers detected over Moscow (and over the 3 high mid-latitude European ionosonde stations in our previous

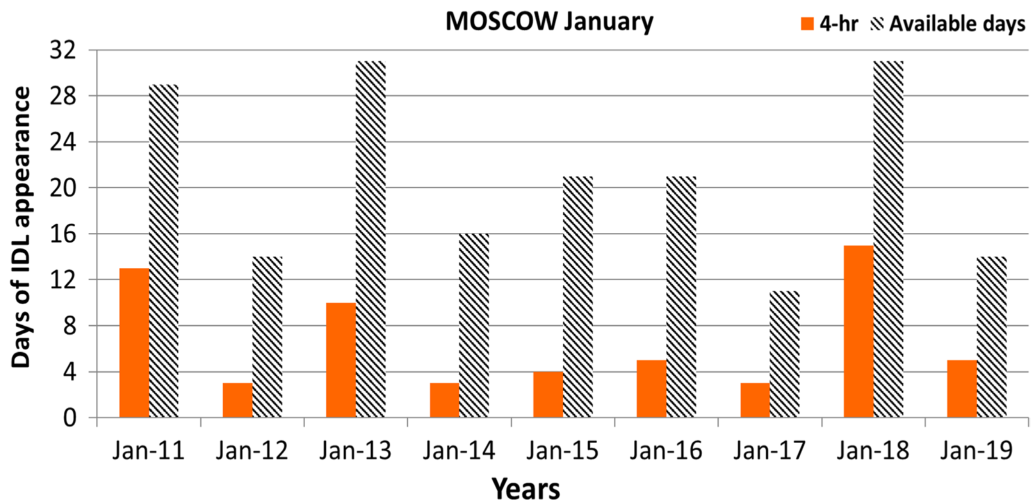

Fig. 6 Histograms showing the occurrence probability of the 4-h periodicity in IDL over Moscow for January, during the period 2011–2019. The number of days with available ionograms is also shown (striped grey colored bars)

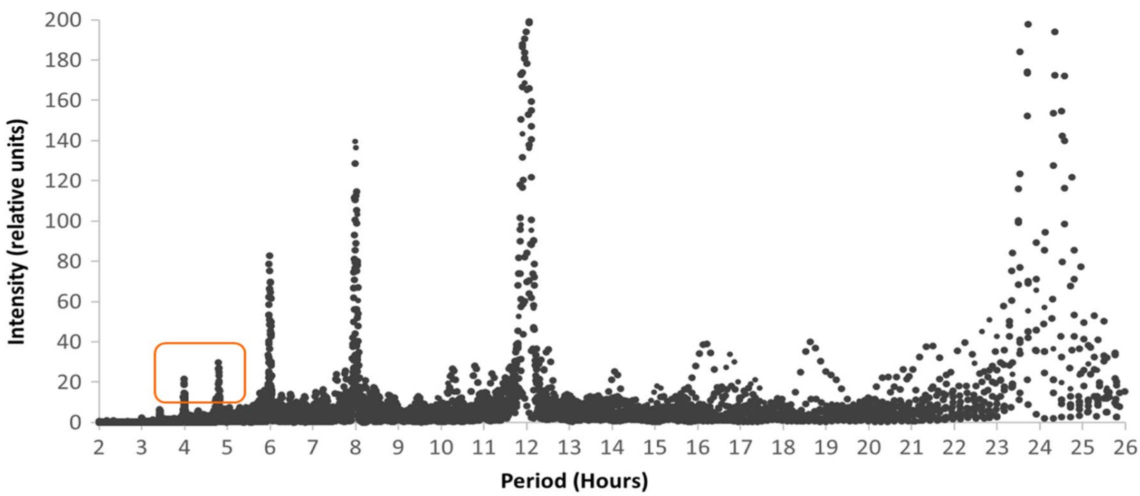

Fig. 7 Lomb periodograms of ionogram numerical data corresponding to IDLs over Moscow. The observed periodicities on Es occurrence for all winter months (December, January, February) during the period 2011–2019 are shown. The 4- and 4.8- hour periodicities are indicated within the orange box

study) primarily during December and January may be attributed to the enhancement of the higher-order atmospheric tides prior to the SSW events. In support to this conclusion, Ma et al. (2022) showed that tidal waves with the same periodicities (mainly 12, 8 and 6-h) may also appear in Total Electron Content(TEC) and they can exhibit a similar response to a SSW event (weaken after SSW onset). They actually reported a TEC response, consistent with He et al. (2020) results after the SSW onset in the year 2018.

Furthermore, there exist very few studies, which report shorter period (4–6 h) tide-like oscillations in ionospheric characteristics over low-latitude regions and have ascribed them to tidal modes of thermospheric winds. In particular, Colerico and Mendillo, (2002) identified a 4–6 h periodicity in the amplitude of zonal and meridional neutral winds in the F region over Peru using a Fabry–Perot interferometer, whereas Lühr and Manoj (2013) based on 10-year CHAMP satellite measurements, provided a complete spectrum of the Equatorial Electrojet (EEJ) variations induced by appreciable higher-order solar migrating tides whose amplitudes maximized around December solstice and equinoxes. Ghodpage et al. (2012) have also demonstrated the prevalence of 4-h

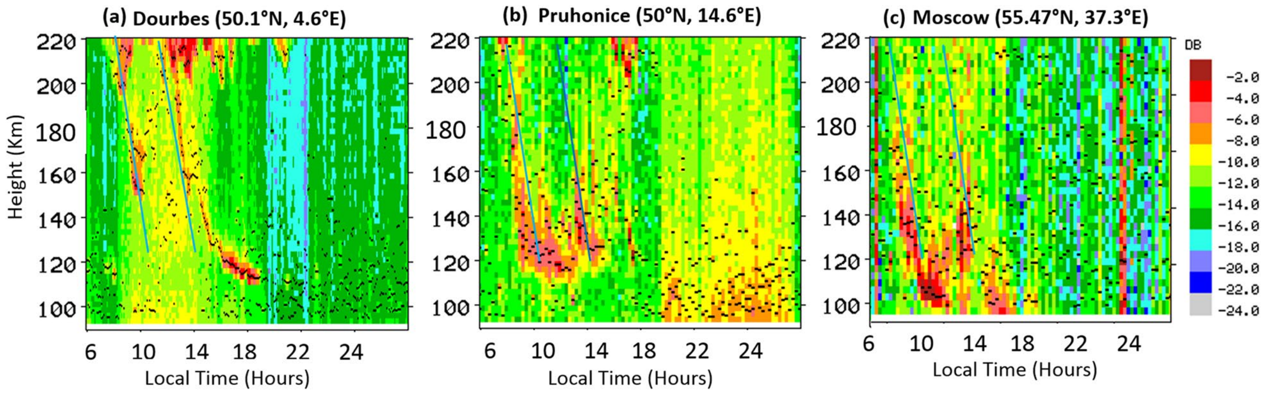

Fig. 8 Daily HTI plots showing a 4-h periodicity of IDL occurrence over **a** Dourbes, **b** Pruhonice and **c** Moscow stations during 31 January 2015. Light blue solid lines are drawn to help the reader identify the IDLs altitude descent

thermospheric tides during winter and around equinoxes with the aid of nocturnal airglow emissions over a low-latitude Indian station.

As evident in the literature results presented above, the shorter-scale periodicities are primarily observed in IDLs and less intermittently in Es occurrence. This can be mainly associated to the fact that in most cases, IDLs are found to suddenly fade out when they decent towards lower heights (~ 120 km), therefore, they cannot contribute to the ionisation enhancement of the Es layers below. As seen in the daily HTI plots in Fig. 4, in some days the IDLs rapidly disappear as they reach lower altitudes (~ 120 km) (Figs. 4a, d, e). This is consistent with results by Earle et al. (2000) who observed the abrupt disappearance of IDLs over Arecibo at lower heights (~ 140 km) which is attributed to the relatively small horizontal wind and shear below 140 km. As explained, the strong wind field at higher altitudes maintains the layer despite the recombination and diffusion effects, whereas at lower altitudes, where the wind decreases, recombination and diffusion cause the layer quickly to disappear. Furthermore, Miyoshi et al., (2009) showed that the amplitude of high-order tidal components in temperature and wind diminish below 150 km.

The evidence presented here demonstrate the possible effect of high-order migrating thermospheric tides primarily during winter months over higher mid-latitude regions. Nevertheless, consideration of additional potential sources of higher-order tidal modes in ionospheric layer characteristics is required before more definitive interpretations about the origin of short-periodicity IDLs can be made. For instance, non-linear interactions between different tides is a possible mechanism for the generation of higher-order tides (Angelats i Coll and Forbes 2002). Zhao et al. (2005) proposed several additional candidate mechanisms of short-time variations, such as the direct thermal excitation by solar heating, the tidal and gravity wave interaction and the modulation of tidal amplitude by planetary waves. Hence, the origin of high-order migrating tides in the thermosphere remains an unresolved issue, and the clarification of the generation mechanisms of higher-order IDL tidal modes will be addressed in future work.

Summary and conclusions

We combined results obtained from two powerful techniques, the HTI method and the Spectrum analysis for an extended period (9 years) to analyze the occurrence, the characteristics and the seasonal variations of IDL and Es over the higher mid-latitude station of Moscow. It is shown that the semidiurnal periodicity in IDL and Es occurrence prevails throughout the year. However, shorter periodicities (8-, 6-, 4.8- and 4-h) in IDL and Es occurrence are found to dominate in certain seasons. A terdiurnal periodicity in IDL is strong during winter and autumn months, while it appears also in summer months only in Es. A quarter-diurnal periodicity in IDL and Es is pronounced during autumn and winter months, nevertheless, is weaker than the terdiurnal periodicity.

For the first time, shorter-scale (4.8- and 4- hour) periodicities mainly in IDL are disclosed over Moscow, which appear in all 9 years, during December and January and occasionally in February and November. This new evidence agrees with the observed 4-h periodicity in three higher mid-latitude stations (Pruhonice, Juliusruh, Dourbes) during winter months, as shown in our earlier study. It should be noted that the four stations have almost the same latitude and are spread within the longitude range 4°E to 37°E, indicating that the observed 4-h periodicity in IDL occurrence represents a large-scale and not a localized phenomenon which persists during winter months. The observed short-scale

IDL periodicity is marked by two distinct descending ionisation layers, which occur within the day, with about 4 h apart, starting from the altitude of 220 km at the local sunrise. The two layers appear at certain times (~ 8 and ~ 12 UT) of the day in all four longitudinally separated stations, indicating that the 4-h oscillation is a westward propagating global structure. Our results suggest that higher-order thermospheric tides (4.8- and 4- hour) are most likely responsible for the formation and evolution of the 4.8- and 4- hour periodicity in IDL and Es.

Through this study, it is shown that the system of thermospheric winds, which is dominated by the action of the semidiurnal, terdiurnal and quarter-diurnal tides (that are responsible for the observed 12-, 8- and 6-h periodicities in IDL and Es, respectively) might consider to incorporate higher-order (4.8- and 4- hour) tides as well, to account for the observed shorter-scale oscillation in the IDL and Es properties.

In conclusion, the current work established that the shorter-scale periodicity (4.8- and 4-h in IDL and Es is a regular, global-scale phenomenon that is most probably linked to higher-order thermospheric tides, which, though they appear weaker than the well-established semidiurnal, terdiurnal and quarter-diurnal tides, they seem to play a key role on the generation of descending layers in higher mid-latitudes during winter months. However, to confirm the possible effect of higher-order thermospheric tides on the creation of shorter-period IDL oscillations, additional investigation is needed, that will include in depth analysis of other potential sources as well, which is out of the scope of the present work. At last, our results concerning shorter-scale periodicities in IDL and Es may also prove useful for future investigations that attempt to explore tidal variability on shorter timescales in the upper atmosphere, which, up to date, are much less understood.

Abbreviations

HTI	Height–time–intensity
IDL	Intermediate descending layer
Es	Sporadic E
WST	Wind shear theory
AGW	Atmospheric gravity waves
RO	Radio occultation
CSES	China Seismo-Electromagnetic Satellite
FORMOSAT–3/COSMIC	FORMOsa SATellite mission-3/Constellation Observing System for Meteorology, Ionosphere and Climate
FY-3C	Fengyun-3C
GNSS	Global Navigation Satellite System
ISR	Incoherent Scatter Radar
DIDBase	Digital Ionogram Database

Acknowledgements
We are grateful of Prof. Christos Haldoupis and Dr. Chis Meek for their valuable contribution on the software development for HTI method.

Author contributions
CO did the data analysis, the figures and wrote the paper. TL applied the Spectrum Analysis. HH applied the HTI analysis and revised the paper. TLG and VAP discussed the results and contributed to revise the paper. All authors read and approved the final manuscript.

Funding
This work is co-funded by: a) the project "Retrospective modelling and prediction of ionospheric weather" —BILATERAL/RUSSIA (RFBR)/1118/0004 which is co-funded by the Republic of Cyprus and the European Regional Development Fund in the frames of RESTART Programme 2016–2020 'Bilateral Collaborations'. In addition, the project was supported by the "RFBR grant 19–52-25001_Kipr_a".

Availability of data and materials
The Moscow station ionograms can be can be found at the DIDBase (Digital Ionogram Database, https://ulcar.uml.edu/DIDBase/) of the Global Ionospheric Radio Observatory (GIRO, http://giro.uml.edu/).

Declarations

Ethics approval and consent to participate
Not applicable.

Consent for publication
Not applicable.

Competing interests
The authors declare that they have no known competing financial interests or personal relationships that could have appeared to influence the work reported in this paper.

Author details
[1]Frederick Research Center, 7 Filokyprou St Palouriotissa, 1036 Nicosia, Cyprus. [2]Frederick University, Nicosia, Cyprus. [3]IZMIRAN, Troitsk, Moscow, Russia.

Received: 12 September 2022 Accepted: 3 March 2023
Published online: 17 March 2023

References
Andoh S, Saito A, Shinagawa H et al (2020) First simulations of day-to-day variability of mid-latitude sporadic E layer structures. Earth Planets Space 72:165
Andoh S, Saito A, Shinagawa H (2022) Numerical simulations on day-to-day variations of low-latitude Es layers at Arecibo. Geophys Res Lett 49:e2021GL097473. https://doi.org/10.1029/2021GL097473
Angelats i Coll M, Forbes JM (2002) Nonlinear interactions in the upper atmosphere: The s = 1 and s = 3 nonmigrating semidiurnal tides. J Geophys Res 107(A8):1157. https://doi.org/10.1029/2001JA900179
Arras C, Jacobi C, Wickert J (2009) Semidiurnal tidal Signature in Sporadic E occurrence rates derived from GPS radio occultation measurements at higher midlatitudes. Ann Geophys 27:2555–2563
Axford WI (1963) The formation and vertical movement of dense ionized layers in the ionosphere due to neutral windshears. J Geophys Res Space Phys 68(3):769. https://doi.org/10.1029/JZ068i003p00769
Azeem I, Walterscheid RL, Crowley G, Bishop RL, Christensen AB (2016) Observations of the migrating semidiurnal and quaddiurnal tides from the RAIDS/NIRS instrument. J Geophys Res Space Phys 121:4626–4637. https://doi.org/10.1002/2015JA022240
Bencze P, Buresova D, Lastovicka J, Marcz F (2004) Behaviour of the F1-region, and Es and Spread-F phenomena at European middle latitudes, particularly under geomagnetic storm conditions. COST 271 Action. Effects of the upper atmosphere on terrestrial and Earth-space communications Final Report. Ann Geophys. 47(2–3):1131–1143. https://doi.org/10.4401/ag-3290

Carter LN, Forbes JM (1999) Global transport and localized layering of metallic ions in the upper atmosphere. Ann Geophys 17:190–209. https://doi.org/10.1007/s00585-999-0190-6
Christakis N, Haldoupis C, Zhou Q, Meek C (2009) Seasonal variability and descent of mid-latitude sporadic E layers at Arecibo. Ann Geophys 27(3):923–931. https://doi.org/10.5194/angeo-27-923-2009
Colerico MJ, Mendillo M (2002) The current state of investigations regarding the thermospheric midnight temperature maximum (MTM). J Atmos Sol Terr Phys 64:1361–1369
Didebulidze GG, Dalakishvili G, Todua M (2020) Formation of Multilayered Sporadic E under an Influence of Atmospheric Gravity Waves (AGWs). Atmosphere 11:653. https://doi.org/10.3390/atmos11060653
Earle GD, Bishop RL, Collins SC, González SA, Sulzer MP (2000) Descending layer variability over Arecibo. J Geophys Res Space Phys 105(A11):24951–24961. https://doi.org/10.1029/2000JA000029
Forbes JM (1995) Tidal and planetary waves. In: Johnson RM, Killeen TL (eds) The Upper Mesosphere and Lower Thermosphere: a review of experiment and theory. American Geophysical Union, Washington, DC
Forbes JM, Vial F (1989) Monthly simulations of the solar semidiurnal tide in the mesosphere and lower thermosphere. J Atmos Terr Phys 51:649–661. https://doi.org/10.1016/0021-9169(89)90063-9
Gan C, Hu J, Luo X, Xiong C, Gu S (2022) Sounding of sporadic E layers from China Seismo-Electromagnetic Satellite (CSES) radio occultation and comparing with ionosonde measurements. Ann Geophys 40:463–474. https://doi.org/10.5194/angeo-40-463-2022
Ghodpage RN, Siingh D, Singh RP et al (2012) Tidal and gravity waves study from the airglow measurements at Kolhapur (India). J Earth Syst Sci 121:1511–1525. https://doi.org/10.1007/s12040-012-0240-4
Haldoupis C (2012) Midlatitude sporadic E. A typical paradigm of atmosphere–ionosphere coupling. Space Sci Rev 168:441–461. https://doi.org/10.1007/s11214-011-9786-8
Haldoupis C, Pancheva D (2006) Terdiurnal tide like variability in sporadic E layers. J Geophys Res Space Phys. https://doi.org/10.1029/2005JA011522
Haldoupis C, Pancheva D, Mitchell NJ (2004) A study of tidal and planetary wave periodicities present in midlatitude sporadic E layers. J Geophys Res. https://doi.org/10.1029/2003JA010253
Haldoupis C, Meek C, Christakis N, Pancheva D, Bourdillon A (2006) Ionogram height–time intensity observations of descending sporadic E layers at mid-latitude. J Atmos Sol - Terr Phys 68:539. https://doi.org/10.1016/j.jastp.2005.03.020
Haldoupis C, Haralambous H, Meek C (2020) On the necessity of using foμEs instead of foEs in estimating the intensity and variability of sporadic E layers. J Atmos Sol-Terr Phys 206(2):105327. https://doi.org/10.1016/j.jastp.2020.105327
Haldoupis C, Pancheva D, Singer W, Meek C, MacDougall J (2007) An explanation for the seasonal dependence of midlatitude sporadic E layers J Geophys Res: Space Phys 112(A6). https://doi.org/10.1029/2007JA012322
He M, Forbes JM, Chau JL, Li G, Wan W, Korotyshkin DV (2020) High-order solar migrating tides quench at SSW onsets. Geophys Res Lett 47:e2019GL086778. https://doi.org/10.1029/2019GL086778
Jacobi C (2012) 6 year mean prevailing winds and tides measured by VHF meteor radar over Collm (51.31°N, 13.01°E) J. Atmos. Sol.-Terr. Phys 78:8–18. https://doi.org/10.1016/j.jastp.2011.04.010
Jacobi C, Fytterer T (2012) The 8-h tide in the mesosphere and lower thermosphere over Collm (51.31°N, 13.01°E), 2004–2011. Adv Radio Sci 10:265–270. https://doi.org/10.5194/ars-10-265-2012
Kumari K, (2021a) Short-Term Variability of Atmospheric Tides in Earth's Mesosphere and Lower Thermosphere Region. All Dissertations. 2814. https://tigerprints.clemson.edu/all_dissertations/2814
Lee C-C, Liu J-Y, Pan C-J, Hsu H-H (2003) The intermediate layers and associated tidal motions observed by a digisonde in the equatorial anomaly region. Ann Geophy 21:1039–1045. https://doi.org/10.5194/angeo-21-1039-2003
Li G, Ning B, Patra A, Abdu M, Chen J, Liu L, Hu L (2013) On the linkage of daytime 150 km echoes and abnormal intermediate layer traces over Sanya. J Geophys Res Space Phys 118:7262–7267. https://doi.org/10.1002/2013JA019462
Liu G, Janches D, Lieberman RS, Moffat-Griffin T, Fritts DC, Mitchell NJ (2020) Coordinated observations of 8- and 6-hr tides in the mesosphere and lower thermosphere by three meteor radars near 60°S latitude. Geophys Res Lett 47:e2019GL086629. https://doi.org/10.1029/2019GL086629
Lühr H, Manoj C (2013) The complete spectrum of the equatorial electrojet related to solar tides: CHAMP observations. Ann Geophys 31(8):1315–1331. https://doi.org/10.5194/angeo-31-1315-2013
Ma H, He M, Liu L, Li W, Yang Y, Zhang R et al (2022) Solar tide-like signatures in the ionospheric total electron content during the 2018 sudden stratospheric warming event. Space Weather 20:e2022SW003042. https://doi.org/10.1029/2022SW003042
MacDougall JW (1974) 110 km neutral zonal wind patterns. Planet Space Sci 22:545
MacDougall JW, Jayachandran P (2005) Sporadic E at cusp latitudes. J Atmos Sol Terr Phys 67:1419–1426. https://doi.org/10.1016/j.jastp.2005.07.011
MacDougall J, Jayachandran P, Plane J (2000) Polar cap Sporadic-E: part 1, observations. J Atmos Sol Terr Phys 62:1155–1167. https://doi.org/10.1016/S1364-6826(00)00093
Maeda J, Heki K (2014) Two-dimensional observations of midlatitude sporadic E irregularities with a dense GPS array in Japan. Radio Sci 49:28–35. https://doi.org/10.1002/2013RS005295
Maksyutin SV, Sherstyukov ON, Fahrutdinova AN (2001) Dependence of sporadic – E layer and lower thermosphere dynamics on solar activity. Adv Space Res 27(6–7):1265–1470. https://doi.org/10.1016/S0273-1177(01)00195-8
Mathews JD (1998) Sporadic E: current views and recent progress. J Atmos Sol Terr Phys 60:413. https://doi.org/10.1016/0021-9169(93)90080-I
Mathews JD, Morton YT, Zhou Q (1993) Observations of ion layer motions during the AIDA campaign. J Atmos Sol Terr Phys 55(3):447–457. https://doi.org/10.1016/0021-9169(93)90080-I
Miyoshi Y, Fujiwara H, Forbes JM, Bruinsma SL (2009) Solar terminator wave and its relation to the atmospheric tide. J Geophys Res 114:A07303. https://doi.org/10.1029/2009JA014110
Morton YT, Mathews JD, Zhou Q (1993) Further evidence for a 6-h tide above Arecibo. J Atmos Sol Terr Phys 55:459–465. https://doi.org/10.1016/0021-9169(93)90081-9
Mošna Z, Koucká Knížová P, Potužníková K (2015) Coherent structures in the Es layer and neutral middle atmosphere. J Atmos Sol Terr Phys 136:155–162. https://doi.org/10.1016/j.jastp.2015.06.007
Niranjan K, Srivani B, Naidu VVS (2010) Daytime descending intermediate layers observed over a sub-tropical Indian station Waltair during low-solar activity period. Ann Geophys 28:807–815. https://doi.org/10.5194/angeo-28-807-2010
Oberheide J, Forbes JM, Zhang X, Bruinsma SL (2011) Climatology of upward propagating diurnal and semidiurnal tides in the thermosphere. J Geophys Res Space Phys. https://doi.org/10.1029/2011JA016784
Oikonomou C, Haralambous H, Haldoupis C, Meek C (2014) Sporadic E tidal variabilities and characteristics observed with the Cyprus Digisonde. J Atmos Sol Terr Phys 119:173–183. https://doi.org/10.1016/j.jastp.2014.07.014
Oikonomou C, Haralambous H, Leontiou T, Tsagouri I, Buresova D (2022) Mošna, Z (2022) Intermediate descending layer and sporadic E tidelike variability observed over three mid-latitude ionospheric stations. Adv Space Res 69(1):96–110. https://doi.org/10.1016/j.asr.2021.08.038
Osterman GB, Heelis RA, Bailey GJ (1994) Modeling the formation of intermediate layers at Arecibo latitudes. J Atmos Sol Terr Phys 99(A6):11357–11365. https://doi.org/10.1029/94JA00519
Patra AK (2011) Descending ion layer property in the Gadanki radar observations of 150 km echoes and its implication to the echoing phenomenon. J Geophys Res. https://doi.org/10.1029/2011JA016805
Pezzopane M, Pignalberi A, Pietrella M (2015) On the influence of solar activity on the mid-latitude sporadic E layer. J Space Weather Space Clim. https://doi.org/10.1051/swsc/2015031
Pietrella M, Bianchi C (2009) Occurrence of sporadic-E layer over the ionospheric station of Rome: analysis of data for thirty-two years. Adv Space Res 44:72–81. https://doi.org/10.1016/j.asr.2009.03.006
Pietrella M, Pezzopane M, Bianchi C (2014) A comparative sporadic-E layer study between two mid-latitude ionospheric stations. Adv Space Res 54:150–160. https://doi.org/10.1016/j.asr.2014.03.019
Pignalberi A, Pezzopane M, Zuccheretti E (2014) Sporadic E layer at mid-latitudes: average properties and influence of atmospheric tides. Ann Geophys 32:1427–1440. https://doi.org/10.5194/angeo-32-1427-2014

Press WH, Teukolsky SA, Vetterling WT, Flannery BP (2007) Least-squares frequency analysis of unequally spaced data numerical recipes, Third Edition, Lomb, NR. Astrophys Space Sci 39:447–462
Qiu L, Zuo X, Yu T, Sun Y, Liu H, Sun L, Zhao B (2021) The characteristics of summer descending sporadic E layer observed with the ionosondes in the China region. J Geophys Res Space Phys. https://doi.org/10.1029/2020JA028729
Reinisch BW, Galkin IA, Khmyrov GM, Kozlov AV, Lisysyan IA, Bibl K, Cheney G, Kitrosser D, Stelmash S, Roche K, Luo Y, Paznukhov VV, Hamel R (2008) Advancing Digisonde technology: the DPS-4D, In radio sounding and plasma physics. AIP Conf Proc 974:127–143. https://doi.org/10.1063/1.2885023
Resende LCA, Zhu Y, Arras C, Denardini CM, Chen SS, Moro J, Barros D, Chagas RAJ, Da Silva LA, Andrioli VF et al (2022) (2022) Analysis of the Sporadic-E Layer Behavior in Different American Stations during the Days around the September 2017 Geomagnetic Storm. Atmosphere 13:1714. https://doi.org/10.3390/atmos13101714
Rowe JR (1974) Downward transport of nighttime Es-layers into the lower E-region at Arecibo. J Atmos Solar Terr Phys 36:225–234
Saito S, Hosokawa K (2021) Study of structures of the sporadic E layer by using dense GNSS network observations. Navigation 68:751–758. https://doi.org/10.1002/navi.454
Santos AM, Batista IS, Abdu MA, Humberto J, Sobral JHA, Souza JR, Brum CGM (2019) Climatology of intermediate descending layers (or 150km echoes) over the equatorial and low-latitude regions of Brazil during the deep solar minimum of 2009. Ann Geophys 37:1005–1024. https://doi.org/10.5194/angeo-37-1005-2019
Santos AM, Batista IS, Sobral JHA, Brum CGM, Abdu MA, Souza JR (2020) Some differences in the dynamics of the intermediate descending layers observed during periods of maximum and minimum solar flux. J Geophys Res Space Phys. https://doi.org/10.1029/2019JA027682
Santos ÂM, Brum CGM, Batista IS, Sobral JHA, Abdu MA, Souza JR (2022) Responses of intermediate layers to geomagnetic activity during the 2009 deep solar minimum over the Brazilian low-latitude sector. Ann Geophys 40:259–269. https://doi.org/10.5194/angeo-40-259-2022
Shinagawa H, Tao C, Jin H, Miyoshi Y, Fujiwara H (2021) Numerical prediction of sporadic E layer occurrence using GAIA. Earth Planets and Space. https://doi.org/10.1186/s40623-020-01330-y
Smith AK, Ortland DA (2001) Modeling and analysis of the structure and generation of the terdiurnal tide. J Atm Sci 58:3116–3134
Smith AK, Pancheva DV, Mitchell NJ (2004) Observations and modeling of the 6-hour tide in the upper mesosphere. J Geophys Res. https://doi.org/10.1029/2003JD004421
Taylor MJ, Pendleton WR, Gardner CS, States RJ (1999) Comparison of terdiurnal tidal oscillations in mesospheric OH rotational temperature and Na lidar temperature measurements at mid-latitudes for fall/spring conditions. Earth Planet Space 51:877. https://doi.org/10.1186/BF03353246
Tong Y, Mathews JD, Ying WP (1988) An upper E region quarter diurnal tide at Arecibo? J Geophys Res. https://doi.org/10.1029/JA093iA09p10047
Voiculescu M, Haldoupis C, Schlegel K (1999) Evidence for planetary wave effects on midlatitude back scatter and sporadic E layer occurrence. Geophys Res Lett 26:1105. https://doi.org/10.1029/1999GL900172
Walterscheid RL, Sivjee GG (1996) Very high frequency tides observed in the airglow over Eureka (80N) Geophys. Res Lett 23:3651–3654
Whitehead JD (1961) The formation of the sporadic E-layer in the temperate zones. J Atmos Solar Terr Phys. https://doi.org/10.1016/0021-9169(61)90097-6
Won Y-I, Wu QY, Cho M, Shepherd GG, Killeen TL, Espy PJ, Kim Y, Solheim B (2003) Polar cap observations of mesospheric and lower thermospheric 4-hour waves in temperature. Geophys Res Lett 30:1377. https://doi.org/10.1029/2002GL016364
Xu X, Luo J, Wang H, Liu H, Hu T (2022) Morphology of sporadic E layers derived from Fengyun-3C GPS radio occultation measurements. Earth Planets Space. https://doi.org/10.1186/s40623-022-01617-2
Yamazaki Y, Richmond DA (2013) A theory of ionospheric response to upward-propagating tides: electrodynamic effects and tidal mixing effects. J Geophys Res Space Phys 118(9):5891–5905. https://doi.org/10.1002/jgra.50487
Yeh WH, Liu JY, Huang CY, Chen SP (2014) Explanation of the sporadic-E layer formation by comparing FORMOSAT-3/COSMIC data with meteor and wind shear information. J Geophys Res Atmos 119(8):4568–4579. https://doi.org/10.1002/2013JD020798
Yu B, Xue X, Yue X, Yang C, Yu C, Dou X, Ning B, Hu L (2019) The global climatology of the intensity of the ionospheric sporadic E layer. Atmos Chem Phys 19:4139–4151. https://doi.org/10.5194/acp-19-4139-2019,2019
Yu B, Scott CJ, Xue X, Yue X, Dou X (2020) Derivation of global ionospheric Sporadic E critical frequency (foEs) data from the amplitude variations in GPS/GNSS radio occultations. R Soc Open Sci 7:200320. https://doi.org/10.1098/rsos.200320
Yusupov KM, Bakhmetieva NV (2021) Sporadic E Layer with a Structure of Double Cusp in the Vertical Sounding Ionogram. Atmosphere 12:1093. https://doi.org/10.3390/atmos12091093
Zhao G, Liu L, Ning B et al (2005) The terdiurnal tide in the mesosphere and lower thermosphere over Wuhan (30°N, 114°E). Earth Planet Sp 57:393–398. https://doi.org/10.1186/BF03351823

Publisher's Note